

Reentrant metallicity in the Hubbard model: the case of honeycomb nanoribbons

F. Manghi^{1,2,*} and F. Petocchi¹

¹*Dipartimento di Fisica, Università di Modena e Reggio Emilia, Via Campi 213/A, I-41125 Modena, Italy*

²*CNR - Institute of NanoSciences - S3*

Based on the Cluster Perturbation solution of the Hubbard hamiltonian for a 2-D honeycomb lattice we present quasiparticle band structures of nanoribbons at half filling as a function of the on-site electron-electron repulsion. We show that, at moderate values of e-e interaction, ribbons with armchair-shaped edges exhibit an unexpected semimetallic behavior, recovering the original insulating character only at larger values of U .

PACS numbers: 71.30.+h, 73.22.Pr, 71.27.+a, 71.10.Fd

The effect of the many-body interaction in the electronic properties of materials has been one of the most important topics in solid state research over the last decades. Even if in many systems electrons behave as independent (quasi)particles and can be successfully described by standard band theory, the interpretation of the electronic properties of a wide class of materials requires improvements over the single particle approximation. In these cases the repulsive interaction among electrons is responsible of the failure of single particle picture and of the opening/widening of energy gaps. The Hubbard model is the paradigm to describe this phenomenon: sufficiently large values of the on-site e-e repulsion inhibit the inter-site hopping favoring in this way an insulating behaviour. The 1-atom thick 2D honeycomb lattice (graphene) does not contradict this picture: many body effects due to on-site Coulomb repulsion have been shown to lead, for sufficiently strong interactions, to semimetal-to-insulator transition^{1,2} as well as to other deviations from Fermi-liquid behavior such as unconventional quasiparticle lifetimes³, long-range antiferromagnetic order⁴ and spin liquid phase⁵.

In this paper we show that for honeycomb nanoribbons the repulsive e-e interaction may be responsible of a metallic phase in ribbons that in the single particle picture are semiconducting. This appears to be another extraordinary property of the honeycomb lattice.

It is well known that honeycomb nanoribbons manifest peculiar properties related to the topology of their edges⁶: according to single-particle theory ribbons with armchair shaped edges may exhibit a finite energy gap depending on their width⁷⁻⁹, while ribbons with zigzag edges are metallic and become insulating only after the inclusion of an antiferromagnetic order^{10,11}. The modifications of the single particle band structure of zigzag graphene ribbons due to e-e interaction has been investigated within a mean field solution of the Hubbard model^{12,13}, showing spin polarization of edge states and gap opening at the Fermi level. The effects of long-range Coulomb interactions on the electronic states of zigzag and armchair ribbons have been studied by bosonization techniques^{14,15}. How the single particle band picture evolves to a quasi-particle one and how the electronic states of both armchair and zigzag honeycomb ribbons

are modified by short-range on-site Coulomb repulsion described as a true many body term is the question we address in this paper.

The possibility that e-e correlation can cause a metallic behavior in band insulators has been rather controversial and only recently Dynamical Mean Field Theory (DMFT)^{16,17} and Quantum Monte Carlo¹⁸ approaches have been applied to study model band insulators showing that the band gap may be suppressed by e-e repulsion. Here we address this issue in a specific class of systems - honeycomb ribbons - that in the absence of correlation may exhibit either metallic or semiconducting behavior depending on their edge topology. This seems an ideal situation to study how e-e repulsion may - *ceteris paribus* - either open or suppress a gap.

We have adopted a many body approach based on the Cluster Perturbation Theory¹⁹ (CPT). CPT belongs to the class of Quantum Cluster theories^{20,21} that solve the problem of many interacting electrons in an extended lattice by a *divide-and-conquer* strategy, namely solving first the many body problem in a subsystem of finite size and then embedding it within the infinite medium. Quantum Cluster theories represent some of the most powerful tools for the numerical investigation of strongly correlated many-body systems. They include Dynamical Cluster Approach²², Cellular Dynamical Mean Field Theory²³ as well as CPT and have found a unified language within the variational scheme²⁴ based on the the Self Energy Functional approach²⁵. CPT has many interesting characteristics and gives access to non trivial many body effects in a relatively simple way: it exactly reproduces the limits $U/t = 0$ (non-interacting band limit), $U/t = \infty$ (atomic limit); for intermediate values of U/t it opens a gap in metallic systems at half occupation²⁶ and it recovers most of the characteristics of the exact solution of the 1-dimensional case^{19,27}; finally it is relatively easy to implement and, at least for simplest systems, without much numerical effort. In its variational form^{24,28} (Variational Cluster Approximation (VCA)) it can be applied to systems with spontaneously broken symmetry describing antiferromagnetism²⁹ and superconductivity^{30,31}. In zigzag honeycomb ribbons VCA has been applied to study the transition from topological to antiferromagnetic insulator³². CPT shares the

strategy of cluster embedding with other approaches that have been developed to study transport in nanoscopic structures^{33–36} or the metal-insulator transition of the Hubbard model³⁷.

I. CPT FOR HONEYCOMB RIBBONS

In CPT¹⁹ the lattice is seen as the periodic repetition of identical clusters and the Hubbard Hamiltonian is written as the sum of two terms, an intra-cluster (\hat{H}_c) and an inter-cluster one (\hat{V})

$$\hat{H} = \sum_l \hat{H}_l + \sum_{l \neq l'} \hat{H}_{ll'} = \hat{H}_c + \hat{V} \quad (1)$$

where the summations are over all the clusters and

$$\begin{aligned} \hat{H}_l &= -t \sum_{ij\sigma} \hat{c}_{il\sigma}^\dagger \hat{c}_{jl\sigma} + U \sum_i \hat{c}_{il\uparrow}^\dagger \hat{c}_{il\uparrow} \hat{c}_{il\downarrow}^\dagger \hat{c}_{il\downarrow} \\ \hat{H}_{ll'} &= -t \sum_{ij\sigma} \hat{c}_{il\sigma}^\dagger \hat{c}_{j'l'\sigma} \end{aligned}$$

Since in the Hubbard model the e-e Coulomb interaction is on-site, the inter-cluster hamiltonian \hat{V} is single particle and the many body term is present in the intra-cluster hamiltonian \hat{H}_c only, a key feature for the practical implementation of the method. Having partitioned the Hamiltonian in this way we may write the resolvent operator \hat{G} as $\hat{G}^{-1} = z - \hat{H}_c - \hat{V} = \hat{G}^c{}^{-1} - \hat{V}$ and from this

$$\hat{G} = \hat{G}^c + \hat{G}^c \hat{V} \hat{G} \quad (2)$$

The one-particle propagator

$$\begin{aligned} \mathcal{G}(\mathbf{k}n\omega) &= \langle \Psi_0 | \hat{c}_{\mathbf{k}n}^\dagger \hat{G} \hat{c}_{\mathbf{k}n} | \Psi_0 \rangle \\ &+ \langle \Psi_0 | \hat{c}_{\mathbf{k}n} \hat{G} \hat{c}_{\mathbf{k}n}^\dagger | \Psi_0 \rangle \end{aligned}$$

is obtained exploiting the transformation from localized to Bloch basis

$$\hat{c}_{\mathbf{k}n}^\dagger = \frac{1}{\sqrt{N}} \sum_{il} \alpha_i^n(\mathbf{k})^* e^{-i\mathbf{k} \cdot (\mathbf{R}_l + \boldsymbol{\tau}_i)} \hat{c}_{il}^\dagger \quad (3)$$

and similarly for $\hat{c}_{\mathbf{k}n}$. Here $\alpha_i^n(\mathbf{k})$ are the eigenstate coefficients obtained by a band calculation for a superlattice of L identical clusters, identified by the lattice vectors \mathbf{R}_l , each cluster containing M sites at positions $\boldsymbol{\tau}_i$; n is the band index and the summation is over the $N = L \times M$ lattice sites. We get

$$\mathcal{G}(\mathbf{k}n\omega) = \frac{1}{M} \sum_{ii'} e^{-i\mathbf{k} \cdot (\boldsymbol{\tau}_i - \boldsymbol{\tau}_{i'})} |\alpha_i^n(\mathbf{k})|^2 \mathcal{G}_{ii'}(\mathbf{k}\omega) \quad (4)$$

where $\mathcal{G}_{ii'}(\mathbf{k}\omega)$ is the superlattice Green function, namely the Fourier transform of the Green function in local basis

$$\mathcal{G}_{ii'}(\mathbf{k}\omega) = \frac{1}{L} \sum_{ll'} e^{-i\mathbf{k} \cdot (\mathbf{R}_l - \mathbf{R}_{l'})} \mathcal{G}_{ii'}^{ll'}(\omega) \quad (5)$$

This is the quantity that can be calculated by eq.2

$$\mathcal{G}_{ii'}(\mathbf{k}\omega) = \mathcal{G}_{ii'}^c(\omega) + \sum_j B_{ij}(\mathbf{k}\omega) \mathcal{G}_{j'i'}(\mathbf{k}\omega) \quad (6)$$

where $M \times M$ matrix $B_{ij}(\mathbf{k}\omega)$ is the Fourier transform of $\hat{G}^c \hat{V}$ involving neighboring sites that belong to different clusters. Once the cluster Green function in the local basis $\mathcal{G}_{ii'}^c(\omega)$ has been obtained by exact diagonalization, eq. 6 is solved quite simply by a $M \times M$ matrix inversion at each \mathbf{k} and ω . The quasi particle spectrum is then obtained in terms of spectral function $A(\mathbf{k}\omega)$

$$A(\mathbf{k}\omega) = -\frac{1}{\pi} \sum_n \text{Im} \mathcal{G}(\mathbf{k}n\omega). \quad (7)$$

The key approximation in this derivation is the expression of the complete Green function in terms of Green functions of decoupled clusters and it is important to verify the accuracy of the results by using larger and larger cluster sizes. In practice this procedure is limited by the dimensions of Hilbert space used in the exact diagonalization, dimensions that grow exponentially with the number of sites.

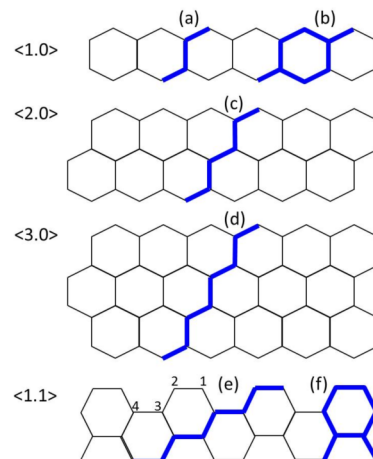


FIG. 1: (Color online) Geometric configurations of honeycomb ribbons with zigzag edges identified according to the notation of reference⁸. The single (a,c) and double (b) chains used to *tile* the extended 1D lattice are also shown.

Fig. 1 illustrates the ribbon geometries and the clusters that are periodically repeated to reproduce both zigzag and armchair ribbons. We want to stress that CPT allows to reproduce the full periodicity of the system of interest and that the ribbons we are describing are extended 1D systems. For the armchair termination in particular we will restrict our analysis to ribbons of small width that in the single particle picture exhibit a large band gap (the band gap in armchair ribbons decreases with width) and as such are the best candidates to manifest the effect we are looking for, namely a band gap suppression induced by e-e repulsion.

II. RESULTS FOR ZIG-ZAG AND ARMCHAIR RIBBONS

In the case of zigzag termination we have considered two different widths and in the case of ribbon $\langle 1.0 \rangle$ we have used both single chain (4 sites) and double chain (8 sites) tilings in order to test the influence of cluster size on the quasiparticle spectrum. In Fig. 2 we show the QP Density Of States (DOS) obtained for a specific value of U/t and the two above mentioned cluster sizes, compared with the corresponding non-interacting DOS. We notice that the main features (peak positions, gap opening) do not depend much on the cluster size. We may therefore confidently use the smallest cluster size in all cases. For armchair terminated ribbons we have used two different kinds of clusters: an 8-site chain (Fig. 1 (e)) and an hexagon with two legs (Fig. 1 (f)). As we will show below the cluster shape does not modify the overall picture.

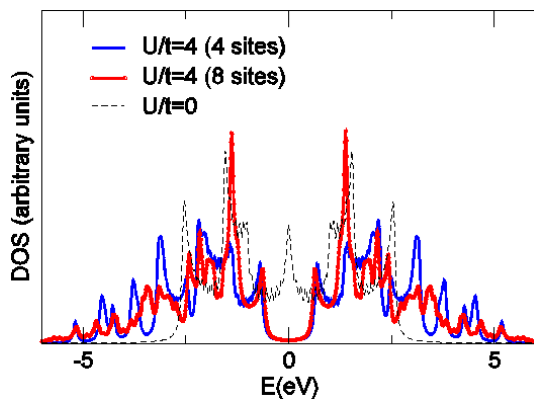


FIG. 2: (Color online) Density of Quasi Particle states obtained for $U/t = 4$ for a zigzag terminated ribbon assuming different cluster sizes (Fig 1 a,b) compared with non-interacting DOS.

As a result of the inclusion of e-e interaction extra structures appear in the quasi particle spectrum below (above) filled (empty); this is what happens also in real materials where Hubbard correlation may be responsible of severe energy renormalization, quasiparticle quenching^{38,39} and the appearance of short lived satellites structures⁴⁰. The main effect of Hubbard correlation however is the opening, for sufficiently strong interaction $U \geq U_c$, of a well defined gap. This is due to the well known Mott-Hubbard mechanism: U inhibits double occupancies of sites and in this way makes electron hopping from site to site less and less energetically favorable, driving the system across a metal-to-insulator transition. This is what happens in model systems at half occupation and in real materials⁴¹. As shown in Fig. 3 the value of U_c for zigzag ribbons depends on the ribbon width: $U_c \simeq 1., 1.52$, for ribbons $\langle 1.0 \rangle, \langle 2.0 \rangle, \langle 3.0 \rangle$ respectively. Previous VCA calculations³² have found for wider ribbons $U_c \approx 3t$, a results not too far from the present one taking into account the larger ribbon width

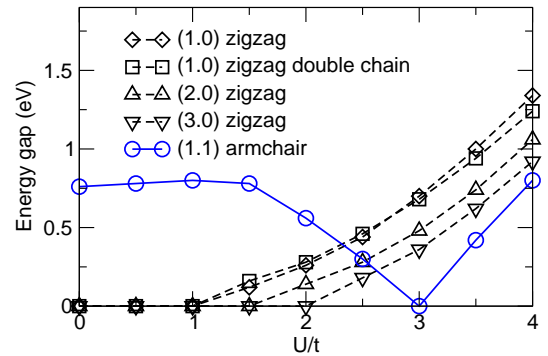


FIG. 3: (Color online) Value of the energy gap as a function of U/t showing a drastically different behavior in zigzag and armchair ribbons. For zigzag termination results obtained for different cluster sizes (single and double chain, Fig. 1 (a) and (b)) and for different ribbon widths are shown.

and the variational procedure used in that work. Recent ab-initio estimate of the screened on-site Coulomb interaction in graphene⁴² provides values of the the same order ($U/t \sim 3.5$).

For the armchair terminated ribbons the situation is completely different. As previously mentioned, according to single particle theory ribbons with armchair shaped edges may be metallic or insulating depending on their width⁷⁻⁹. In particular the ribbon of interest here exhibits a finite gap in the non-interacting picture and we may expect the one-site e-e interaction to reinforce this insulating behavior enlarging the gap. This, surprisingly enough, is not quite the case: switching on e-e correlation the gap first diminishes, reaches zero at $U/t = 3$, and only after that grows linearly with U/t (Fig. 3). At $U = U_c$ the QP band dispersion (Fig. 4) becomes linear around $\mathbf{k} = 0$ and the system semimetallic.

Fig. 3 and 4 report the results obtained for armchair ribbons assuming the tiling showed in Fig. 1 (e). These results are not significantly affected by the shape of the cluster: adopting cluster (f) of Fig. 1 the curve describing the behaviour of the gap versus U/t (Fig. 5) maintains the same remarkable characteristics, with a slightly different critical value U_c . Also the QP band dispersions obtained at the respective U_c , (Fig.4 (c) and inset of Fig. 5) are quite similar.

We may look at the character of quasiparticle states by considering the local spectral function, namely $A(\mathbf{k}, i, \omega) = -\frac{1}{\pi} \sum_n \text{Im} \mathcal{G}(\mathbf{k}n\omega) | \alpha_i^n(\mathbf{k}) |^2$ reported in Fig. 6. We notice that the effect of e-e repulsion is to delocalize states close to the gap region that for $U/t = 0$ are localized either at the edges or in the inner part of the ribbon. In particular for $U/t = 3$ the localization of gapless states responsible of the semimetallic behavior is equally distributed across the ribbon.

We have found that it is possible to reproduce the same gapless band dispersion with the same delocalized character in a single particle picture attributing different hopping terms to edge sites and to inner ones: this is shown

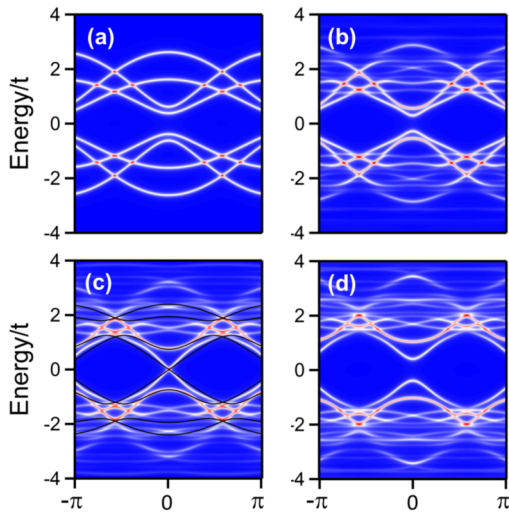


FIG. 4: (Color online) Quasiparticle band structure for armchair terminated ribbon $\langle 1,1 \rangle$ obtained with $U/t = 0$ (a), $U/t = 2$ (b), $U/t = 3$ (c), $U/t = 4$ (d). The black line superimposed in (c) is the band structure obtained in the single particle picture assuming different hopping terms (see text).

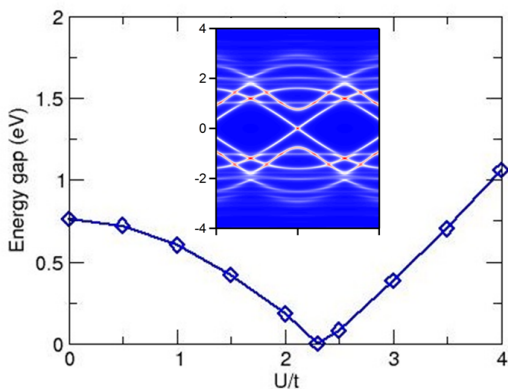


FIG. 5: (Color online) Value of the energy gap as a function of U/t for ribbon $\langle 1,1 \rangle$ obtained with cluster (f) of Fig. 1. The quasiparticle band structure at the critical value $Uc/t = 2.3$ is shown in the inset.

in Fig. 4(c) where we plot the single particle band structure obtained assuming hopping between edge states exactly twice as big as hopping between inner ones. In this sense the net effect of the on-site e-e repulsion is to renormalize the inter-site hopping selectively across the ribbon and to make hopping between doubly coordinated sites (edge sites) more favorable than hopping between sites with triple coordination (inner sites). The gap closing would then be due to a mechanism similar to a mechanical strain. The analogy between mechanical strain, e-e repulsion and magnetic field as responsible of gap tuning in graphene has been recently investigated^{43,44} showing in particular that in the mean field approximation a

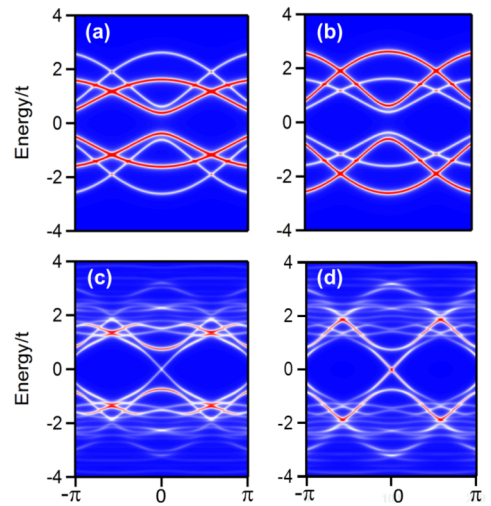


FIG. 6: (Color online) Local spectral functions (see text) for ribbon $\langle 1,1 \rangle$. Top (bottom) panels report the results for $U/t = 0$ ($U/t = 3$); panels (a) and (c) describe the contribution of edge sites (site 1 and 2 of Fig(1) while panels (b), ((d) describe the contribution of innermost sites (site 3 and 4 of Fig. 1).

local nearest neighbor Coulomb interaction may create in a 2D honeycomb lattice non trivial magnetic configurations and metallic phases with broken time reversal symmetry⁴⁴. In the present study we have shown that on-site Coulomb repulsion if treated as a full many body term may induce a semimetallic behavior in a semiconducting 1D honeycomb lattice.

What is surprising is that the Hubbard interaction has opposite effects in the two types of honeycomb ribbons: it *opens* a gap in the metallic ribbon and *closes* it in the semiconducting one. A similar behavior has been reported in a recent paper on correlation effects in topological insulators³². Starting from an extended 2D honeycomb lattice made semiconducting by intrinsic spin-orbit (SO) interaction within the so-called Kane-Mele model⁴⁵, the authors show that for $U/t = 3$ the existing gap closes down. We have repeated the calculation using the same SO parameter and calculated also in this case the gap as a function of U/t . The results are shown in Fig. 7 for a 2D honeycomb lattice with and without SO and again in the semiconducting system we find a regime of U/t where the energy separation between filled and empty states decreases and the pre-existing gap closes down to zero. And this even if the original semiconducting behavior has a completely different physical origin (SO interaction in 2D instead of armchair termination in 1D).

III. CONCLUSIONS

We have calculated the QP band structure of honeycomb nanoribbons solving the Hubbard Hamiltonian within the Cluster Perturbation Theory. We have found

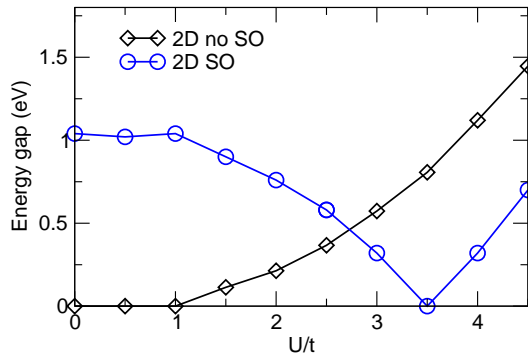


FIG. 7: (Color online) Energy gap as a function of U/t for 2D honeycomb lattice with (circles) and without spin-orbit (diamonds) interaction.

that many body effects associated to local e-e repulsion may be responsible of a (semi)metallic phase in systems with honeycomb lattice. The Hubbard mechanism that inhibits double occupancies of sites, instead of reducing the ability of electrons to jump from site to site, induces a selective renormalization of inter-site hopping and the energy separation between filled and empty states becomes zero at a specific k-point. This behavior appears to be characteristic of honeycomb topology - or perhaps more generally of bipartite lattices - at half occupation and suggests the existence of an U -dependent additional symmetry⁴⁶. Electrons trapped in artificial lattices with honeycomb geometry⁴⁷ are the best candidates where this anomalous behavior induced by e-e repulsion (gap closing/opening for semiconducting/metallic systems) can be experimentally verified.

* Electronic address: franca.manghi@unimore.it

- ¹ A. Liebsch, Phys. Rev. B **83**, 035113 (2011), URL <http://link.aps.org/doi/10.1103/PhysRevB.83.035113>.
- ² W. Wu, Y.-H. Chen, H.-S. Tao, N.-H. Tong, and W.-M. Liu, Phys. Rev. B **82**, 245102 (2010), URL <http://link.aps.org/doi/10.1103/PhysRevB.82.245102>.
- ³ J. González, F. Guinea, and M. A. H. Vozmediano, Phys. Rev. Lett. **77**, 3589 (1996), URL <http://link.aps.org/doi/10.1103/PhysRevLett.77.3589>.
- ⁴ T. Paiva, R. T. Scalettar, W. Zheng, R. R. P. Singh, and J. Oitmaa, Phys. Rev. B **72**, 085123 (2005), URL <http://link.aps.org/doi/10.1103/PhysRevB.72.085123>.
- ⁵ Z. Y. Meng, W. Lang, T. C., F. F. S. Assaad, and A. Muramatsu, Nature **464**, 847 (2010).
- ⁶ A. H. Castro Neto, F. Guinea, N. M. R. Peres, K. S. Novoselov, and A. K. Geim, Rev. Mod. Phys. **81**, 109 (2009), URL <http://link.aps.org/doi/10.1103/RevModPhys.81.109>.
- ⁷ K. Nakada, M. Fujita, G. Dresselhaus, and M. S. Dresselhaus, Phys. Rev. B **54**, 17954 (1996), URL <http://link.aps.org/doi/10.1103/PhysRevB.54.17954>.
- ⁸ M. Ezawa, Phys. Rev. B **73**, 045432 (2006), URL <http://link.aps.org/doi/10.1103/PhysRevB.73.045432>.
- ⁹ L. Brey and H. A. Fertig, Phys. Rev. B **73**, 235411 (2006), URL <http://link.aps.org/doi/10.1103/PhysRevB.73.235411>.
- ¹⁰ Y.-W. Son, M. L. Cohen, and S. G. Louie, Phys. Rev. Lett. **97**, 216803 (2006), URL <http://link.aps.org/doi/10.1103/PhysRevLett.97.216803>.
- ¹¹ L. Pisani, J. A. Chan, B. Montanari, and N. M. Harrison, Phys. Rev. B **75**, 064418 (2007), URL <http://link.aps.org/doi/10.1103/PhysRevB.75.064418>.
- ¹² J. Fernández-Rossier, J. J. Palacios, and L. Brey, Phys. Rev. B **75**, 205441 (2007), URL <http://link.aps.org/doi/10.1103/PhysRevB.75.205441>.
- ¹³ A. Yamashiro, Y. Shimoi, K. Harigaya, and K. Wakabayashi, Phys. Rev. B **68**, 193410 (2003), URL <http://link.aps.org/doi/10.1103/PhysRevB.68.193410>.
- ¹⁴ M. Zarea and N. Sandler, Phys. Rev. Lett. **99**, 256804 (2007), URL <http://link.aps.org/doi/10.1103/PhysRevLett.99.256804>.
- ¹⁵ M. Zarea, C. Büsser, and N. Sandler, Phys. Rev. Lett. **101**, 196804 (2008), URL <http://link.aps.org/doi/10.1103/PhysRevLett.101.196804>.
- ¹⁶ A. Garg, H. R. Krishnamurthy, and M. Randeria, Phys. Rev. Lett. **97**, 046403 (2006), URL <http://link.aps.org/doi/10.1103/PhysRevLett.97.046403>.
- ¹⁷ M. Sentef, J. Kuneš, P. Werner, and A. P. Kampf, Phys. Rev. B **80**, 155116 (2009), URL <http://link.aps.org/doi/10.1103/PhysRevB.80.155116>.
- ¹⁸ N. Paris, K. Bouadim, F. Hebert, G. G. Batrouni, and R. T. Scalettar, Phys. Rev. Lett. **98**, 046403 (2007), URL <http://link.aps.org/doi/10.1103/PhysRevLett.98.046403>.
- ¹⁹ D. Sénéchal, D. Perez, and M. Pioro-Ladrière, Phys. Rev. Lett. **84**, 522 (2000), URL <http://link.aps.org/doi/10.1103/PhysRevLett.84.522>.
- ²⁰ C. Gros and R. Valentí, Phys. Rev. B **48**, 418 (1993), URL <http://link.aps.org/doi/10.1103/PhysRevB.48.418>.
- ²¹ T. Maier, M. Jarrell, T. Pruschke, and M. H. Hettler, Rev. Mod. Phys. **77**, 1027 (2005), URL <http://link.aps.org/doi/10.1103/RevModPhys.77.1027>.
- ²² M. H. Hettler, A. N. Tahvildar-Zadeh, M. Jarrell, T. Pruschke, and H. R. Krishnamurthy, Phys. Rev. B **58**, R7475 (1998), URL <http://link.aps.org/doi/10.1103/PhysRevB.58.R7475>.
- ²³ S. S. Kancharla, B. Kyung, D. Sénéchal, M. Civelli, M. Capone, G. Kotliar, and A.-M. S. Tremblay, Phys. Rev. B **77**, 184516 (2008), URL <http://link.aps.org/doi/10.1103/PhysRevB.77.184516>.
- ²⁴ M. Potthoff, M. Aichhorn, and C. Dahnken, Phys. Rev. Lett. **91**, 206402 (2003), URL <http://link.aps.org/doi/10.1103/PhysRevLett.91.206402>.
- ²⁵ M. Potthoff, Eur. Phys. J. B **32**, 245110 (2003).
- ²⁶ F. Manghi, Journal of Physics: Condensed Matter **26**, 015602 (2014), URL <http://stacks.iop.org/0953-8984/26/i=1/a=015602>.
- ²⁷ M. Potthoff, M. Aichhorn, and C. Dahnken, Phys. Rev. Lett. **91**, 206402 (2003), URL <http://link.aps.org/doi/10.1103/PhysRevLett.91.206402>.
- ²⁸ M. Balzer, W. Hanke, and M. Potthoff, Phys. Rev. B **77**, 045133 (2008), URL <http://link.aps.org/doi/10.1103/PhysRevB.77.045133>.

- PhysRevB.77.045133.
- ²⁹ C. Dahnken, M. Aichhorn, W. Hanke, E. Arrigoni, and M. Potthoff, Phys. Rev. B **70**, 245110 (2004), URL <http://link.aps.org/doi/10.1103/PhysRevB.70.245110>.
- ³⁰ M. Aichhorn, E. Arrigoni, M. Potthoff, and W. Hanke, Phys. Rev. B **74**, 024508 (2006), URL <http://link.aps.org/doi/10.1103/PhysRevB.74.024508>.
- ³¹ D. Sénéchal, P.-L. Lavertu, M.-A. Marois, and A.-M. S. Tremblay, Phys. Rev. Lett. **94**, 156404 (2005), URL <http://link.aps.org/doi/10.1103/PhysRevLett.94.156404>.
- ³² S.-L. Yu, X. C. Xie, and J.-X. Li, Phys. Rev. Lett. **107**, 010401 (2011), URL <http://link.aps.org/doi/10.1103/PhysRevLett.107.010401>.
- ³³ V. Ferrari, G. Chiappe, E. V. Anda, and M. A. Davidovich, Phys. Rev. Lett. **82**, 5088 (1999), URL <http://link.aps.org/doi/10.1103/PhysRevLett.82.5088>.
- ³⁴ M. A. Davidovich, E. V. Anda, C. A. Büsser, and G. Chiappe, Phys. Rev. B **65**, 233310 (2002), URL <http://link.aps.org/doi/10.1103/PhysRevB.65.233310>.
- ³⁵ E. V. Anda, C. Büsser, G. Chiappe, and M. A. Davidovich, Phys. Rev. B **66**, 035307 (2002), URL <http://link.aps.org/doi/10.1103/PhysRevB.66.035307>.
- ³⁶ G. Chiappe and J. A. Verges, Journal of Physics: Condensed Matter **15**, 8805 (2003).
- ³⁷ G. Chiappe, C. Büsser, E. V. Anda, and V. Ferrari, Journal of Physics: Condensed Matter **11**, 5237 (1999).
- ³⁸ S. Monastera, F. Manghi, C. A. Rozzi, C. Arcangeli, E. Wetli, H.-J. Neff, T. Greber, and J. Osterwalder, Phys. Rev. Lett. **88**, 236402 (2002), URL <http://link.aps.org/doi/10.1103/PhysRevLett.88.236402>.
- ³⁹ J. Sánchez-Barriga, J. Fink, V. Boni, I. Di Marco, J. Braun, J. Minár, A. Varykhalov, O. Rader, V. Bellini, F. Manghi, et al., Phys. Rev. Lett. **103**, 267203 (2009), URL <http://link.aps.org/doi/10.1103/PhysRevLett.103.267203>.
- ⁴⁰ F. Manghi, V. Bellini, and C. Arcangeli, Phys. Rev. B **56**, 7149 (1997), URL <http://link.aps.org/doi/10.1103/PhysRevB.56.7149>.
- ⁴¹ M. Imada, A. Fujimori, and Y. Tokura, Rev. Mod. Phys. **70**, 1039 (1998), URL <http://link.aps.org/doi/10.1103/RevModPhys.70.1039>.
- ⁴² T. O. Wehling, E. Şaşoğlu, C. Friedrich, A. I. Lichtenstein, M. I. Katsnelson, and S. Blügel, Phys. Rev. Lett. **106**, 236805 (2011), URL <http://link.aps.org/doi/10.1103/PhysRevLett.106.236805>.
- ⁴³ F. Guinea, K. M. I., and G. A. K., Nature Phys. **6**, 30 (2010).
- ⁴⁴ E. V. Castro, A. G. Grushin, B. Valenzuela, M. A. H. Vozmediano, A. Cortijo, and F. de Juan, Phys. Rev. Lett. **107**, 106402 (2011), URL <http://link.aps.org/doi/10.1103/PhysRevLett.107.106402>.
- ⁴⁵ M. Z. Hasan and C. L. Kane, Rev. Mod. Phys. **82**, 3045 (2010), URL <http://link.aps.org/doi/10.1103/RevModPhys.82.3045>.
- ⁴⁶ E. H. Lieb (1993), <http://arxiv.org/abs/cond-mat/9311033>.
- ⁴⁷ A. Singha, M. Gibertini, B. Karmakar, S. Yuan, M. Polini, G. Vignale, M. I. Katsnelson, A. Pinczuk, L. Pfeiffer, K. West, et al., Science **332**, 1176 (2011).